MEASUREMENT AND ANALYSIS OF STIFFNESS PROPERTIES IN MOVING PAPER USING NONCONTACT LASER ULTRASONICS

J.H. Jong, P.H. Brodeur and J.P. Gerhardstein

Institute of Paper Science and Technology
500 10th St. NW, Atlanta, GA 30318 USA

ABSTRACT

An experimental investigation has been conducted to measure real time paper stiffness properties on moving paper using noncontact laser ultrasonics. The generation and detection of Lamb waves by laser ultrasonics were performed previously on static paper to relate the wave phase velocity with the corresponding paper stiffness [1,2]. The current study is focused on the detection and analysis of the two fundamental Lamb wave modes, A_0 and S_0, on moving paper, using photo-induced electromotive force (Photo-EMF) interferometer technology [3]. As the Lamb waves propagated in the plane of paper from the generation point, the two wave modes, A_0 and S_0, were detected in the signal. Each mode represented different stiffness properties of paper. The S_0 mode is a fast-moving fundamental dilatational mode and is used to predict longitudinal stiffness properties in any direction with respect to MD. The A_0 mode is dispersive and is sensitive to out-of-plane shear stiffness properties at high frequency while the low frequency A_0 mode is mostly related to bending stiffness. The A_0 mode analysis is performed using an analyzing technique described by Jong et al. [2]. A new approach to resolve a correction of phase angle at low frequency is also suggested. The analysis is performed using the results obtained by a copy paper sample (80 g/m^2). Nevertheless, the analysis technique should be applicable to other paper grades. The sample was tested above production speeds using a web simulator developed at the Institute of Paper Science and Technology. The experimental results show that the use of on-line laser ultrasonic method is a promising technology to predict real time paper stiffness properties.

INTRODUCTION

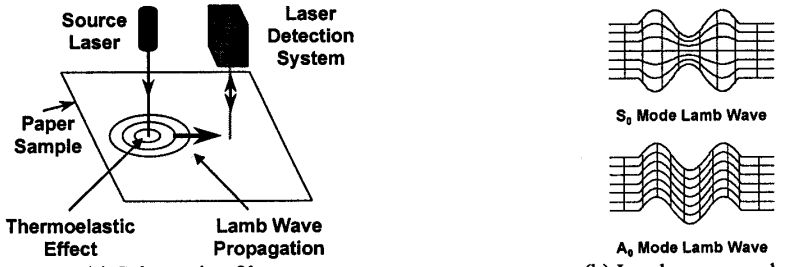

(a) Schematic of laser concept (b) Lamb wave modes

Figure 1. Laser ultrasonics principles [1].

Figure 1 (a) illustrates the process of using noncontact laser ultrasonics to detect wave propagation and correlate wave speeds with paper stiffness properties on moving paper. As the paper moves at production speed, a source laser is used to generate waves in the thermoelastic regime. As the waves propagate in the paper, an interferometric laser detection system is used to detect the waves. Since paper is a relatively thin material, plate Lamb wave propagation theory applies and the fundamental waves A_0 and S_0 are generally observed as shown by Figure 1 (b). Assuming that paper is an orthotropic material, that is, a material that has three mutually orthogonal symmetry planes, relationships between the properties of paper stiffness and wave velocities may be found. [4] The symmetric S_0 mode is non-dispersive in the low frequency region, and a time-of-flight method is used to determine the longitudinal stiffness. On the other hand, the anti-symmetric A_0 mode is dispersive and is used to evaluate the shear stiffness properties in the MD-ZD and CD-ZD plane directions and possibly bending stiffness. Somewhat independent of detection technique, bending is easier to propagate because of large out-of-plane motion at low frequency. As the web speed increases, the level of noise increases and the A_0 mode tends to be the only visible signal due to large amplitudes. Therefore, more emphasis is given to the A_0 mode analysis.

THEORETICAL PREDICTIONS OF PHASE VELOCITIES USING DISPERSION EQUATIONS

The theory of Lamb waves applied to the analysis of paper stiffness has been studied over the last two decades [5,6,7,8,9]. The theory prescribes that a relationship, known as the dispersion equation, between frequency and phase velocity must be satisfied for a Lamb wave to be present in paper. It is in the following form:

$$\frac{\tan(k_{z+} \cdot h_{1/2})}{\tan(k_{z-} \cdot h_{1/2})} = \left[\frac{H_- \cdot G_+}{H_+ \cdot G_-}\right]^{\pm 1} \tag{1}$$

where $h_{1/2}$ is the half thickness of paper, $k_{z\pm}$, $H_\pm$ and $G_\pm$ are functions of frequency, f, wave velocity, c, and some elastic constants that are properties of paper. The wave motion at a particular mode can be predicted by choosing f and c that can satisfy the dispersion equation. The symmetric modes correspond to the solutions of the dispersion equation with a +1 exponent, while the antisymmetric modes correspond to those with a −1 exponent. A complete derivation of the dispersion equation is found in the study by Habeger et al. [5], who also simplified the dispersion equation applicable in the low frequency limit. For the two lowest modes, S_0 and A_0, the simplified relations are

$$c = \sqrt{\frac{Q_{11}}{\rho}} \text{ or } \sqrt{\frac{Q_{22}}{\rho}} \qquad \text{for } S_0 \text{ mode} \tag{2}$$

$$c = \left[2\pi \cdot f \cdot h_{1/2} \cdot \sqrt{\frac{Q_{11}}{3\rho}}\right]^{1/2} \text{ or } \left[2\pi \cdot f \cdot h_{1/2} \cdot \sqrt{\frac{Q_{22}}{3\rho}}\right]^{1/2} \qquad \text{for } A_0 \text{ mode} \tag{3}$$

where Q_{11} *and* Q_{22} are the planar stiffnesses in MD and CD and are the ratios of stress to strain with no out-of-plane stresses and no lateral in-plane strain, ρ is the apparent density of paper (kg/m^3), $h_{1/2}$ is the half thickness of paper (m), f is the frequency (Hz) and c is the wave phase velocity (m/s).

The dispersion equation was numerically solved for copy paper in Figure 2. The elastic stiffness constants used to solve the equation were measured using in-plane and out-of-plane contact ultrasonic methods at the Institute of Paper Science and Technology. The concept of this method is well described. [9]. Each wave mode is identified by a letter (S for symmetric and A for antisymmetric) followed by a number of the order. At very high frequency, all wave modes tend to approach an asymptotic value [10]. This asymptotic value is known to be a Rayleigh wave velocity. The Rayleigh wave exists on the surface of a half-space material. C_{44} or C_{55} is sensitive to the Rayleigh velocity. The cut-off frequency at the S_0 mode is sensitive to C_{33}.

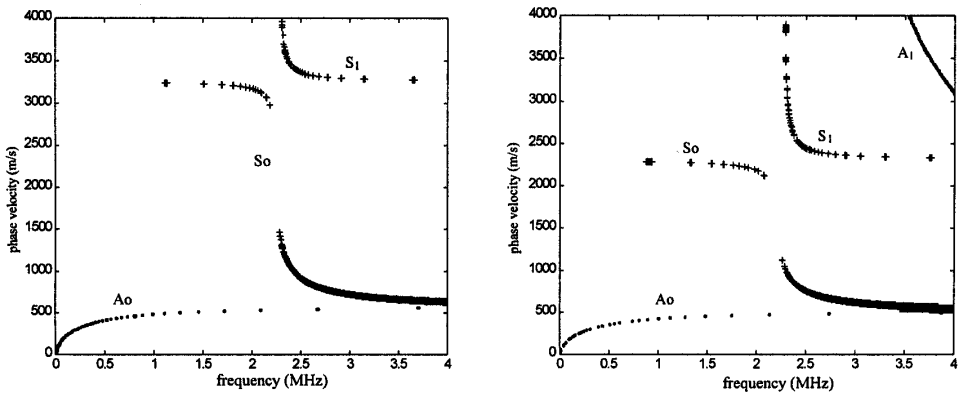

(a) Solutions for copy paper in MD (b) Solutions for copy paper in CD

Figure 2. Dispersion curves of copy paper in MD and CD

RESULTS

Various wave signals collected using an unoptimized Photo-EMF setup at different web speeds are shown in Figure 3 (a) for copy paper in CD and corresponding FFT spectra in (b). The generation system used was a Q-switched Nd:YAG laser at the wavelength of 1064 nm (Near Infrared). The pulse width is 5-7 ns. The maximum energy per pulse was 420 mJ. The beam was focused into a spot size of 1 mm or less to generate high frequency acoustic waves. The distance between a generation point and a detection point was 10 mm. The power of the detection laser was maintained at 1.33 W. The energy level of the source laser was 25.6 mJ using a line generation scheme. The incident angle of the detection beam was at 45 degrees with respect to the normal surface, and the damage by the laser beam to the paper surface was almost nonexistent and invisible to the naked eye near thermoelastic regime.

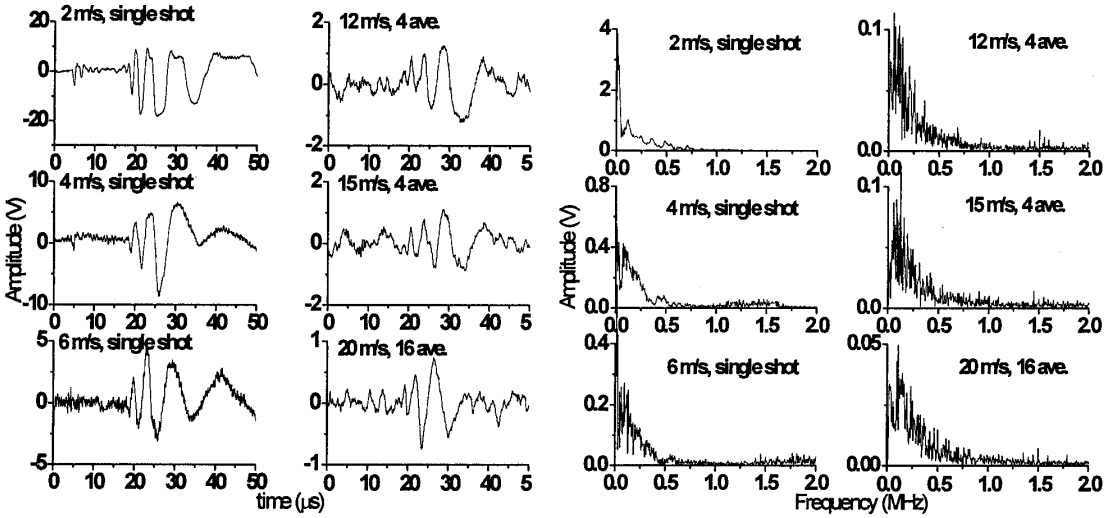

(a) Signals (b) Corresponding FFT spectra

Figure 3. Preliminary results on copy paper in CD for different web speeds: Averaging is minimized to reflect realistic operating conditions.

Figure 3 (a) and (b) show a number of important phenomena observed during the trials. First, as the web speed increases, the signal-to-noise ratio (SNR) decreases significantly. This creates a problem when attempting to detect the waveform, especially the S_0 wave, which is much smaller in amplitude than the A_0 wave. The figure shows that the existence of the S_0 wave becomes obscure as the web speed reaches 10 m/s. Further optimization and fine-tuning of the laser optics is required to enhance SNR. Second, the A_0 mode can still be detected at 20 m/s, which is higher than typical production speed of 18.5 m/s for copy paper [11]. This implies that the A_0 mode analysis is important to relate real time paper stiffness properties with on-line control of the papermaking machine to produce better paper. Third, the FFT spectra show that the energy is mostly present in the low frequency region below 0.5 MHz. Therefore, the A_0 mode analysis is limited to the low frequency region only. For a thin paper such as copy paper, this prevents us from obtaining the out-of-plane shear stiffness properties in MD-ZD and CD-ZD plane directions (C_{44} and C_{55}), because the A_0 phase velocity does not reach a plateau yet. This is verified from the dispersion curves in Figure 2 (b). On the other hand, the out-of-plane shear stiffness can be evaluated for a thick paper such as linerboard, which reaches a plateau rather quickly in the low frequency region [8].

DISCUSSION OF DATA ANALYSIS TECHNIQUE

The low frequency S_0 mode wave can be analyzed in a straightforward manner by using a cross-correlation technique due to its nondispersive characteristics [2,5,6,10]. On the other hand, the interpretation of the A_0 mode is difficult because the phase velocity increases with frequency. A data analysis technique has been developed to evaluate the dispersive A_0 signal with a correction term for unwrapped phase angle [2]. The technique is based on an approach originally proposed by Sachse and Pao [12] and later implemented to Lamb waves by Schumacher et al.

[13]. The reader is encouraged to read the study by Jong et al. for details of the A_0 mode analysis technique [2]. In short, two signals are detected at two different distances between generation and detection. The A_0 portion of the signals are extracted, zero-padded and windowed using a rectangular window. Then, FFT spectrum is obtained for each signal along with unwrapped phase angles. The difference between the phase angles is computed and applied to Eq. 4 to calculate the A_0 phase velocity.

$$c = \frac{-2\pi \cdot f \cdot \Delta d}{(\Delta\phi + 2m\pi)} \tag{4}$$

where c is the phase velocity of the A_0 mode (m/s), f is the frequency (Hz), Δd is the difference between two generation/detection distances (m), $\Delta\phi$ is the difference in unwrapped phase angle for a given frequency (rad), and m is an integer for correction of the phase at lower frequency. The correction term is necessary because the unwrapped phase angle is calculated from low to high frequencies. A discontinuity existed in the signal at very low frequency due to the limit on sampling rate and time duration. A small error resulting from the cut-off of a low frequency signal may build up and generate an overestimation of the A_0 phase velocity at higher frequency [2,6]. The error may be reduced or avoided if the distance between generation and detection is very close or if the signal can be analyzed for sufficient time to pick up the low frequency A_0 mode components.

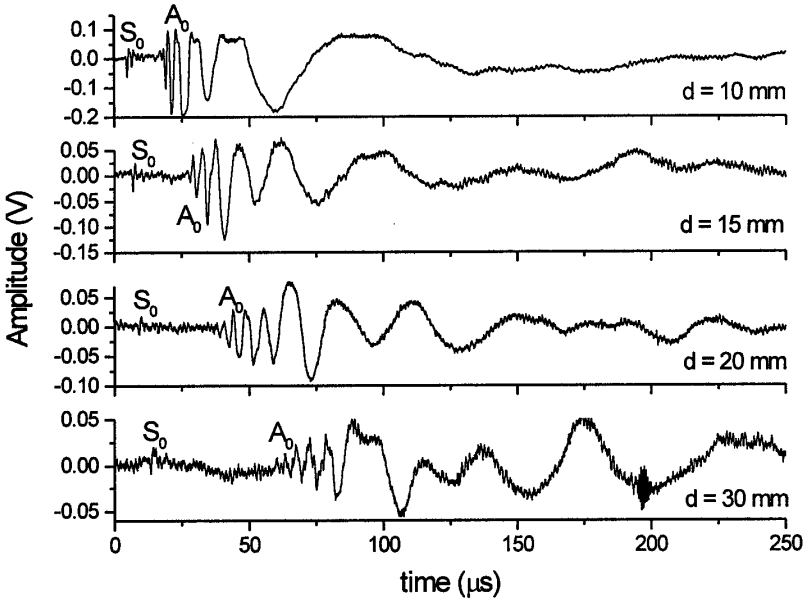

Figure 4. Comparison of Lamb waves for different distances between generation and detection in copy paper in CD at 2 m/s: All signals were obtained using a single shot. The power of detection laser was maintained at 1.33 W. The energy level of source laser was 25.6 mJ using a line generation in near-thermoelastic mode.

To analyze the effect of generation/detection distance on moving paper, Figure 4 is plotted to compare the propagation of S_0 and A_0 waves in copy paper in CD. Four distances at 10mm, 15mm, 20mm and 30mm were chosen to determine the effect on signal attenuation and propagation. Also, to observe both A_0 and S_0 waves, the signals obtained at 2 m/s were selected as opposed to high speed cases where S_0 was not obvious.

First, let us focus on the effect of generation/detection distance on S_0 mode. Figure 5 shows the magnified region of S_0 waves obtained in Figure 4. It is clear that the SNR decreases as the generation/detection distance increases. Also, by comparing FFT spectra of each S_0 wave, it can be found that the main frequency peak slightly shifted to the lower frequency. This is consistent with observations at static paper. By using the cross-correlation technique of two signals among all four distances, relative time delays can be computed between them. The resulting S_0 wave velocities are calculated in Table 1.

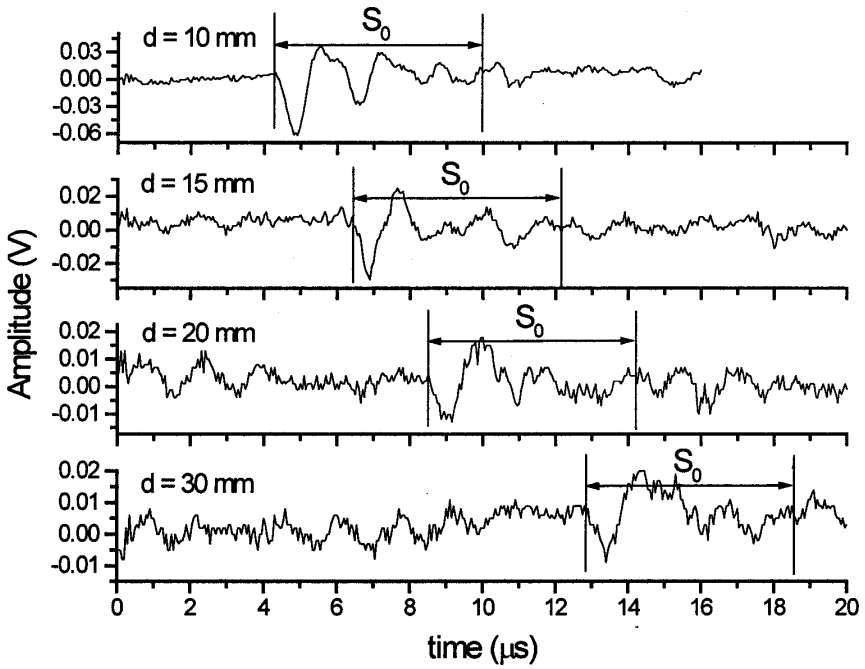

Figure 5. Comparison of S_0 mode signals obtained at different distances using 2 m/s web speed in Figure 4.

Table I. Cross-correlation of the S_0 signals at different generation/detection distances for 2 m/s in CD of copy paper

Two S_0 signals at two different detection points (mm)	Relative time delay between the two signals indicated by maximum peak of cross-correlation (μs)	S_0 wave velocity using a time-of-flight method (m/s)
d=10 mm & d=15 mm	2.05	2439
d=10 mm & d=20 mm	4.20	2381
d=10 mm & d=30 mm	8.60	2326
d=15 mm & d=20 mm	2.20	2273
d=15 mm & d=30 mm	6.60	2273
d=20 mm & d=30 mm	4.40	2273
Average S_0 velocity		**2327 ± 69.6**

The average S_0 wave velocity of six combinations was determined to be 2327±69.9 m/s. In addition, Table II shows a comparison of S_0 wave velocities and Q_{22} properties obtained by the current noncontact laser ultrasonics and the contact method. The S_0 velocity by the noncontact method is very close to the one obtained by the contact method.

Table II. Comparison of the measured and calculated S_0 wave velocity and the corresponding in the low frequency range below cut-off frequency for copy paper in CD using contact and noncontact laser ultrasonics

Average S_0 wave velocity from the current noncontact laser ultrasonics	2327 ± 69.6 m/s
Measured S_0 wave velocity using a contact laser ultrasonics	2322 ± 24 m/s
Q_{22} based on noncontact laser ultrasonics	4.74 ± 0.29GPa
Q_{22} based on contact laser ultrasonics	4.72 ± 0.11GPa

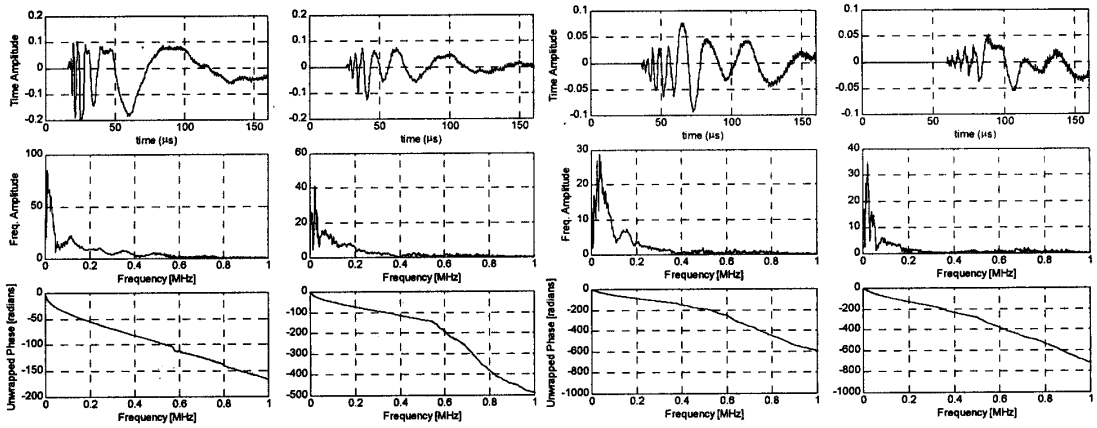

(a) d = 10 mm (b) d = 15 mm (c) d = 20 mm (d) d = 30 mm

Figure 6. A_0 mode analysis of signals

For A_0 mode analysis in moving paper, the A_0 waves in Figure 4 are analyzed using the technique described earlier. Figure 6 (a), (b), (c) and (d) present zero-padded A_0 waves, FFT spectra and unwrapped phase angles for each generation/detection distance at 10 mm, 15 mm, 20 mm and 30 mm, respectively. Based on FFT spectra, the signal energy appears to be present only up to 0.4 MHz. Therefore, the A_0 phase velocity is only valid up to that frequency. Past that frequency, the unwrapped phase angles are no longer valid.

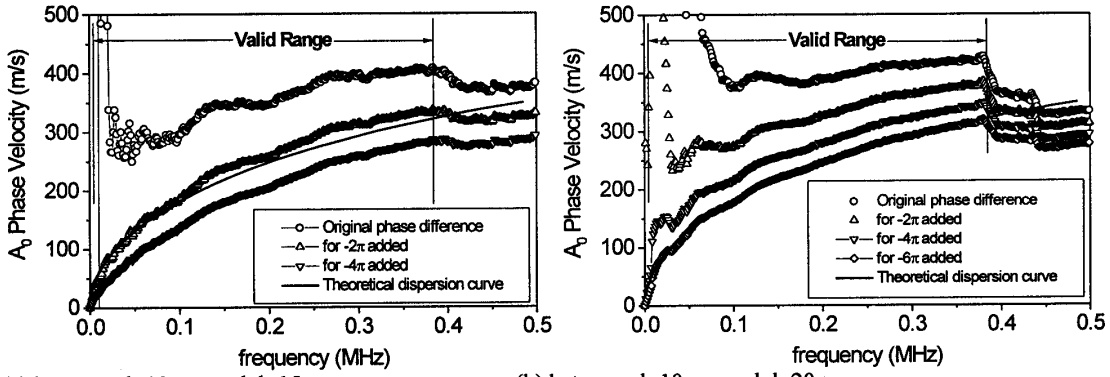

(a) between d=10mm and d=15mm (b) between d=10mm and d=20mm

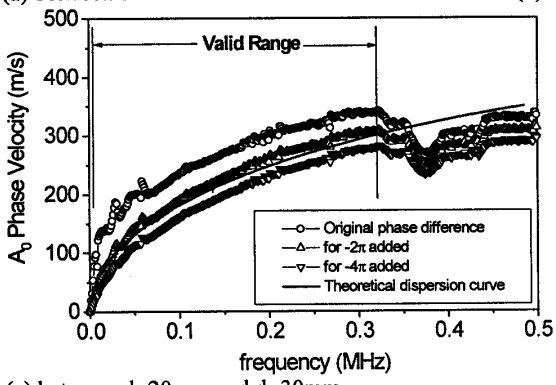

(c) between d=20mm and d=30mm

Figure 7. Comparison of theoretical A_0 dispersion curve to experimental results with corrected phase angles

Figure 7 compares the A_0 dispersion curve with the experimental results corrected for the phase angles at three detection distances. Figures 7 (a), (b) and (c) show the comparison of A_0 velocities for 10&15mm, 10&20mm, and 20&30mm, respectively. The valid range of the signal is shown in the plot and it corresponds to the region where significant energy is present in the FFT spectrum. The original data were corrected for the phase angle differences by -2π, -4π and -6π. Fig. (a) and (c) are best matched with -2π correction, while (b) shows a good prediction with -6π.

Mainly, the problem arises when determining which correction term should be used to predict the right A_0 phase velocity. When the A_0 mode analysis is carried out, the theoretical dispersion curve is typically not available and is subjected to change whenever a papermaking condition is varied slightly. Hence, there is no reference velocity available to determine the right correction angle. To overcome this difficulty, a simple approach was taken to determine the correction term as described in Figure 8. This figure shows that the solid curve approximated by the simplified relation in Eq. 3 is relatively accurate in the very low frequency region until the curve deviates significantly from the theoretical curve. For this particular case of copy paper in CD, the simplified relation has a 5% overestimation from the theoretical prediction at 50 kHz. This proves that the simplified relation may be used as a reference curve in lieu of the theoretical dispersion curve at low frequency.

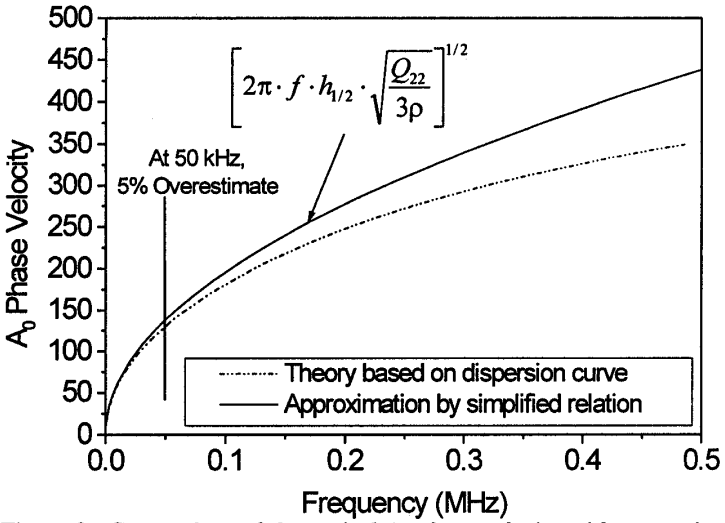

Figure 8. Comparison of theoretical A_0 phase velocity with approximate A_0 phase velocity at low frequency for typical copy paper signals in CD

Let's assume that the 5% overestimation is acceptable to predict a theoretical A_0 curve up to a certain frequency. By combining Eqs. 2, 3 and 4, the phase angle and the correction term can be shown in the following form,

$$\Delta\phi + 2m \cdot \pi = \frac{-\sqrt{2\pi \cdot f} \cdot \Delta d \cdot 3^{1/4}}{\sqrt{h_{1/2} \cdot \sqrt{\frac{Q_{22}}{\rho}}}} \qquad (5)$$

Figure 9 is plotted to show the upper and lower limit of the A_0 phase velocity based on a $\pm\pi$ phase angle limit from the approximate A_0 curve. The $\pm\pi$ phase angle limits for a given frequency were obtained by Eq. 5, which shows a direct relationship between phase angle and frequency for a simplified A_0 mode. To find the A_0 phase velocity limits corresponding to the $\pm\pi$ phase angles, Eq. 4 is used with the $\pm\pi$ phase-shifted angles. Initial phase shift by $-\pi$ would result in a negative A_0 phase velocity between $-\pi$ and 0 and the velocity shoot-up between 0 and $+\pi$. Therefore, this region needs to be avoided. The corresponding frequency for this was up to 3 kHz. For a valid analysis, only the frequency above this frequency should be considered.

This method is introduced based on the assumption that the phase angle can be shifted only by $\pm 2\pi$ and that for a given frequency, there should be only one corrected A_0 velocity that falls within the boundary.

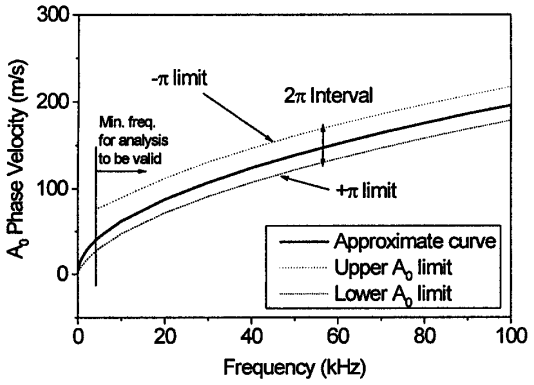

Figure 9. Upper and lower limit of A_0 phase velocity based on $\pm\pi$ phase angle limit

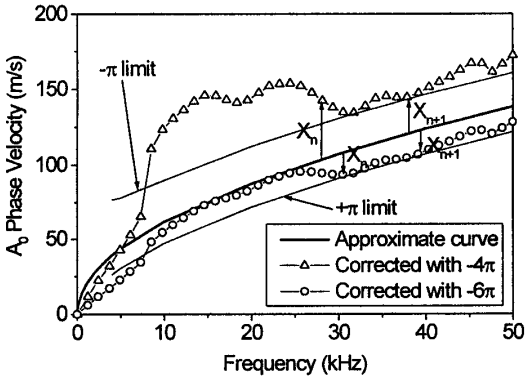

Figure 10. Comparison of the correction terms within upper and lower limits

Finally, in Figure 10, the approximate A_0 curve with $\pm\pi$ phase velocity limits is compared with the correction terms within the low frequency range identified in Figures 8 and 9. For simplicity, a minimum summation of the difference between the approximate curve and each correction curve may be calculated within the allowable frequency region to determine the most probable correction terms. It may be formulated as the following relationship.

$$Min_{difference} = \sum_{n=1}^{n\ at\ allowable\ frequency} \sqrt{\left| x_n^2 - x_{approx}^2 \right|} \qquad (6)$$

where x_n is the phase velocity at a given frequency with a correction term, x_{approx} is the approximate phase velocity at the same frequency and n is the increment of the frequency where a data point exists.

The weakness of this method to determine a proper correction term is that the valid frequency is limited to the small range due to fast deviation of the simplified A_0 curve. For the analysis in copy paper in CD, the valid frequency is between 3 kHz and 50 kHz. It is entirely possible that the majority of the data points fall within the boundary for that low frequency region but at high frequency the data points may be out of the boundary. Further work is required to address some defects of the current method.

CONCLUSIONS

A Photo-EMF interferometer has been successful in demonstrating the detection of real time A_0 mode waves at and above production speeds using a web simulator. The S_0 mode was also detected but limited to the low speed. The samples tested include a light grade such as copy paper and heavy grade such as 42-lb linerboard and bleachboard. The low frequency portion of the A_0 mode was evaluated in terms of phase velocity and frequency. A new approach to resolve a correction of phase angle at low frequency was also suggested. The results show that the on-line laser ultrasonic method is a promising technology for controlling real time paper stiffness properties.

ACKNOWLEDGEMENTS

The authors would like to thank the collaboration of E.F. Lafond from IPST for the setup of laser instruments and the collection of data, C.C. Habeger from IPST for his valuable comments on the manuscript and B.M. Pufahl for the design of the web simulator. Necessary equipment was provided by B. Pouet and M. Klein from Lasson

Technologies. The authors also would like to acknowledge the support of the Member Companies of the Institute of Paper Science and Technology. The authors thank the U.S. Department of Energy, Office of Industrial Technologies through its Agenda 2020 Program for the Pulp and Paper Industry [Cooperative Agreement No. DE-FC07-97ID13578]. However, any opinions, findings, conclusions, or recommendations expressed herein are those of the authors and do not necessarily reflect the views of DOE.

REFERENCES

1. Brodeur, P.H., Johnson, M.A., Berthelot, Y.H. and Gerhardstein, J.P., "Noncontact Laser Generation and Detection of Lamb Waves in Paper," *J. Pulp Paper Sci.* 23(5): J238-J243 (1997)
2. Jong, J.H., Lafond, E.F., Brodeur, P.H., Gerhardstein, J.P. and Pufahl, B.M., "Dispersion of Lamb Waves Propagating in Static and Moving Paper To Measure Stiffness Using Non-Contact Laser Ultrasonics," *Proceedings of 85th Pulp and Paper Technical Association of Canada Annual Meeting*, Montreal, Canada, Jan. 25-29 pp.A145-A148 (1999)
3. Pouet, B., Lafond, E., Pufahl, B., Bacher, D., Brodeur, P. and Klein, M., "On-Machine Characterization of Moving Paper Using a Photo-emf Laser Ultrasonics Method," *Proceedings of SPIE Conference on Process Control and Sensors for Manufacturing*, Newport, CA, SPIE3589:160-169 (1999)
4. Baum, G.A., "Elastic Properties, Paper Quality, and Process Control," *Appita*, 40(4): 288-293 (1987)
5. Habeger, C.C., Mann, R.W. and Baum, G.A., "Ultrasonic Plate Waves in Paper," *Ultrasonics*, 17: 57-62 (1979)
6. Cheng, J.C. and Berthelot, Y.H., "Theory of Laser-generated Transient Lamb Waves in Orthotropic Plates," *J. Phys. D: Appl. Phys.*, 29: 1857-1867 (1996)
7. Johnson, M.A., "Investigation of the Mechanical Properties of Copy Paper Using Laser Generated and Detected Lamb Waves," *Ph.D. Thesis*, Georgia Institute of Technology (1996).
8. Mann, R.W., Baum, G.A. and Habeger, C.C., "Determination of All Nine Orthotropic Elastic Constants for Machine Made Paper," *TAPPI J.* 63(2):164-167 (1980)
9. Habeger, C.C., Van Zummeren, M.L., Wink, W.A., Pankonin, B.M. and Goodlin, R.S., "Using a Robot-based Instrument to Measure the In-plane Ultrasonic Velocities of Paper," *TAPPI J.* 72(7): 171-175 (1989)
10. Viktorov, I.A., "Rayleigh and Lamb Waves," *Plenum Press*, New York (1967)
11. Biermann, C.J., "Essentials of Pulping and Papermaking", *Academic Press Inc.*, London, TS1175 B5 (1993)
12. Sachse, W. and Pao, Y.H., "On the Determination of Phase and Group Velocities of Dispersive Waves," *J. Appl. Phys.*, 49(8): 4320-4327 (1978)
13. Schumacher, N.A., Burger, C.P. and Gien, P.H., "A Laser-based Investigation of High-order Modes in Transient Lamb Waves," *J. Acoust. Soc. Am.* 93(5): 2981-2984 (1993)